Journal of Peptide Science
J. Pept. Sci. 2008; **14**: 697–707
Published online 13 December 2007 in Wiley InterScience (www.interscience.wiley.com). DOI: 10.1002/psc.976

JOURNAL OF PEPTIDE SCIENCE

Functional and structural characterization of apidaecin and its *N*-terminal and *C*-terminal fragments

XU-XIA ZHOU,[a,b] WEI-FEN LI[b] and YUAN-JIANG PAN[a]*

[a] Institute of Chemical Biology and Pharmaceutical Chemistry, Zhejiang University, Zhejiang University Road 38#, Hangzhou, 310027, China
[b] Microbiology Division, College of Animal Science, Zhejiang University, Hangzhou 310027, China

Received 10 October 2007; *Accepted 22 October 2007*

Abstract: Two aspects were studied to elucidate the functional and structural characterization of apidaecin and its *N*-terminal and *C*-terminal fragments: (i) Functions of the *N*-terminal and *C*-terminal fragments of apidaecin were first studied by measuring their antibacterial activity, their ability to enter *Escherichia coli* cells and their effects on the activities of β-galactosidase and alkaline phosphatase. The results indicate that neither the *N*-terminal nor the *C*-terminal of apidaecin contains intracellular delivery unit or active segment. (ii) The effect of apidaecin on the ATPase activity of DnaK, and the interactions of apidaecin with *E.coli* lidless DnaK and DnaK D-E helix were studied. Results showed that apidaecin could interact with the *E.coli* lidless DnaK protein and stimulate its ATPase activity, but not with *E.coli* DnaK D-E helix. This indicated that the antimicrobial activity of apidaecin may be shown by stimulating the ATPase activity of DnaK by binding to its conventional substrate-binding site, to decrease its cellular concentration of DnaK by competing with natural substrates and inhibit the enzymes' activities of *E. coli* cells. It is the first study to suggest that the apidaecin-binding site of DnaK is the conventional substrate binging site.

Keywords: proline-rich peptide; apidaecin; *N*-terminal fragment; *C*-terminal fragment; DnaK; function regions; circular dichroism

INTRODUCTION

Drug resistance is a major obstacle to successful antibacterial chemotherapy. With the emergence of antimicrobial-resistant bacterial strains, the current drug families start to fail, and there is an urgent need for alternative agents, preferably with novel modes of action that will prevent bacteria from mounting a quick response and building resistance. Proline-rich antibacterial peptides, including apidaecins, drosocin and pyrrhocoricin, are potential therapeutic molecules. These peptides are rich in the cationic residues arginine, lysine and histidine, and are proline-rich. They kill bacteria by acting stereospecifically on a bacterial protein through a bacteriostatic rather than a lytic process, and so they are potentially nontoxic to eukaryotic cells and thus suitable for use as systemic drugs [1–5].

Apidaecins are the largest group of proline-rich antimicrobials known. They were the first to be studied in detail with respect to the mechanism and the identity of the amino acid residues responsible for the antibacterial action [1,4–7]. The pharmacophore delivery unit architecture has been proposed to be a general feature of the proline-rich antibacterial peptide family [8,9]. However, despite a wealth of information on the amino acid residues important for function, little is known about the pharmacophore delivery unit architecture of apidaecin. So, in this research, apidaecin and its *N*-terminal and *C*-terminal fragments were synthesized and two aspects were studied to elucidate the functional and structural characterization of apidaecin and its *N*-terminal and *C*-terminal fragments: (i) Functions of the *N*-terminal and *C*-terminal fragments of apidaecin were first studied to elucidate if the two fragments contained intracellular delivery unit or active segment by studying their antibacterial activity, their ability to enter *Escherichia coli* cells and their effects on the activities of β-galactosidase and alkaline phosphatase. (ii) The effect of apidaecin on the ATPase activity of DnaK, and the interactions of apidaecin with *E.coli* lidless DnaK and DnaK D-E helix were studied. The elucidation of the function of apidaecin and its *N*-terminal and *C*-terminal fragments and the interaction between apidaecin and the *E. coli* DnaK or lidless protein will increase our understanding of the structure–function relationships of proline-rich peptides, and this information will be helpful in the design of antimicrobial peptide variants as potential novel therapeutic agents [10–13]. Table 1 gives a list of the synthetic peptides used in this study.

MATERIALS AND METHODS

Peptide Preparation and Fluorescein Labeling

The lidless variant of DnaK (2–517, conventional substrate binging site of DnaK protein) were isolated and

* Correspondence to: Yuan-Jiang Pan, Institute of Chemical Biology and Pharmaceutical Chemistry, Zhejiang University, Zhejiang University Road 38#, Hangzhou, 310027, China; e-mail: yuanjiang_pan@163.com

Table 1 Synthetic peptides used in this study

Peptides	Sequences
Unlabeled apidaecin and its fragments	
Apidaecin Ho^+	GKPRPQQVPPRPPHPRL
AP1-9 (apidaecin *N*-terminal region)	GKPRPQQVP
AP9-17 (apidaecin *C*-terminal region)	PPRPPHPRL
Fluorescein-labeled apidaecin and its fragments	
Fl-K-apidaecin	FITC-KGKPRPQQVPPRPPHPRL
Fl-K-AP1-9	FITC-KGKPRPQQVP
Fl-K-AP9-17	FITC-KPPRPPHPRL
E.coli DnaK D-E helix fragment	
E. coli 583–615	IEAKMQELAQVSQKLMEIAQQQHAQQQTAGADA

The 17-residue peptide (GKPRPQQVPPRPPHPRL) identified as 'Apidaecin Ho^+' comes from the bald-faced hornet, *Dolichovespula maculata* [1].

made free of bound nucleotide, as previously described [14,15] and were maintained in a HEPES buffer (25 mM *N*-(2-hydroxyethyl)piperazine-N0-2-ethanesulfonic acid/50 mM KCl/5 mM MgCl2/5 mM 2-mercaptoethanol at pH 7.0). *N*-terminal 9-flourenylmethyoxycarbonyl (Fmoc)-protected amino acids were used for synthesis of the peptides [16–18]. Peptides were synthesized using Fmoc chemistry on Fmoc–PAL–polyethylene–glycol–polystyrene copolymer resin by a Milligen 9050 continuous-flow automated synthesizer (Applied Biosystems Foster City, USA). An extra lysine residue was added at the *N*-terminus of apidaecin, AP1-9 and AP9-17 to attach the fluorescein moiety. The following side chain protection scheme was used: Asp(OAllyl), His(Trt), Glu(OtBu), Gln(Trt), Ser(tBu), Thr(tBu), Arg(Pbf) and Lys(Alloc). After the chain assembly was completed, the peptide resin was treated with Pd(PPh3)4/PhSiH3 to remove the allyl-protecting groups by following a literature procedure [19]. Fluorescein labeling was conducted while the peptide was still attached to the resin according to Rapaport and Shai [20]. The completion of the reaction was monitored by the ninhydrin assay [21]. After removal of the *N*-terminal Fmoc protection, peptides were cleaved from the resin and purified of HPLC until MALDI-MS revealed a single species with the expected molecular ions. The identity of the peptides was confirmed by electrospray mass spectrometry, using an API I instrument (Perkin Elmer SCIEX).

Antibacterial Efficacy Assay

E. coli K88, *E. coli* BL21, *Staphylococcus aureus, Bacillus subtilis* and *Listeria monocytogenes* were used as indicator bacteria. Antibacterial assays were performed according to Castle *et al.* [1]. In short, exponentially growing bacterial cells were diluted to 1000 CFU/ml in Luria-Bertani (LB) broth and placed into 96-well plates. Peptides were serially diluted and added to the bacteria. The final concentrations of peptides ranged between 0.001 and 10 μg/ml; control wells did not contain peptide. The minimum inhibitory concentration (MIC) was determined by identifying the concentration of peptide that completely inhibited bacterial growth after ~24 h of incubation.

Cell Penetration Assay

To study the ability of apidaecin and its fragments to enter cells, fluorescein-labeled peptides were added to *E. coli* K88 cells at final concentrations of 10 μg/ml for Fl-K-apidaecin, 5.0 μg/ml for Fl-K-AP1-9 and 5.0 μg/ml for Fl-K-AP9-17. The cells were allowed to acquire the substrate for 60 min at 37 °C, the excess substrate was removed and the cells were washed extensively with phosphate-buffered saline (PBS; pH 6.8). The cells were fixed with PBS containing 1% (v/v) paraformaldehyde. A sample of the cell solution was placed onto a slide and a cover-glass was used to obtain an unmovable monolayer of cells. The cells were examined with a Leica TCS SPII laser scanning confocal microscope.

Treatment of the Live *E. coli* Culture

A 5 ml culture was shaken at 37 °C for 5–6 h, then 300 μl was added to 30 ml of LB rich nutrient medium, and the bacterial culture was shaken at 37 °C overnight. Then 5 μl of 6 μg/μl apidaecin solution, 2.5 μl of 6 μg/μl AP1-9 solution or 2.5 μl of 6 μg/μl AP9-17, and 5 μl of 2 μmol/μl apidaecin solution were added to 500 μl of the overnight cultures, respectively, and the mixtures were incubated at 30 °C for 6 h. The cells were harvested by 2 min sonication with a probe sonicator and then centrifuged for 20 min at 3000 *g*. To test the effects of apidaecin, AP1-9 and AP9-17 on the activity of β-galactosidase and alkaline phosphatase, another 500 μl of the overnight culture was harvested before the same concentration of peptide was added. The supernatants were used for the β-galactosidase and alkaline phosphatase assays [8]. The magainin II antimicrobial peptide, which is active against *E.coli* and has been proved to kill cells by 'carpet' mechanism with the bacterial membrane as the main target, was used as the negative control [22]. Magainin II was purchased from Sigma.

Enzymatic Assays

β-Galactosidase. A 50 μl sample of cell lysate was placed into each well of a 96-well plate, 110 μl of 100 mM PBS (pH 7.5) containing 1 mM $MgSO_4$/β-mercaptoethanol (95 : 5, v/v) was added to each well, and the plate was covered and

DOI: 10.1002/psc

incubated at 37 °C for 5 min. A 50 μl portion of a 4 mg/ml *o*-nitrophenyl β-D-galactopyranoside (ONPG) substrate solution was added to each well, and the plate was incubated at 37 °C until the contents of the well were bright yellow. The reaction was terminated by adding 90 μl of 1 M Na_2CO_3, and the plate was scanned at 405 nm by a microtiter dish reader. Enzyme activity is expressed as the molar of ONP released by hydrolysis of ONPG per well per minute.

Alkaline phosphatase. A 50 μl sample of cell lysate was added into each well of a 96-well plate, 110 μl of 1.5 M 2-amino-2-methyl-1-propanol buffer (pH 10.3) was added to each well, and the plate was covered and incubated at 37 °C for 5 min. A 50 μl portion of 4.9 mg/ml *p*-nitrophenyl disodium phosphate substrate solution was added to each well, and the plate was incubated at 37 °C until the contents of the well were bright yellow. The reaction was terminated by addition of 90 μl of a 1 M H_3PO_4, and the plate was scanned at 405 nm by a microtiter dish reader set. Enzyme activity is expressed as the molar of *p*-nitrophenol released by hydrolysis of *p*-nitrophenyl phosphate per well per minute.

ATPase Activity Assay

Recombinant DnaK protein was purchased from StressGen (Victoria, Canada). Phosphate release was assayed by a spectrophotometric method using the EnzChek Phosphate Assay Kit (Molecular Probes, Inc.). The reaction took place in 125 μl of reaction buffer (20 mM Tris–HCl (pH 7.5), 1 mM $MgCl_2$, 0.2 mM sodium azide), with 300 mM ATP (except for assaying the baseline), 5 μg of DnaK, 2-amino-6-mercapto-7-methylpurine ribonucleoside (MESG) and the purine nucleoside phosphorylase recommended by the manufacturer. A concentration of peptide of 500 μM was used to measure the effect of peptides on ATPase activity. The concentration of inorganic phosphate (Pi) was proportional to the absorbance at 360 nm and was calibrated by standard KH_2PO_4 solutions.

Circular Dichroism (CD) Measurements

CD spectra were performed on a Jasco J720 instrument at room temperature in a 0.1 mm path-length cell according to Kragol *et al.* [8]. Doubly distilled water was used as solvent for apidaecin and its fragments. The concentration of peptide was approximately 1.0 mg/ml, and was determined each time by quantitative RP-HPLC [23]. Curves were smoothed by the algorithm provided by Jasco. Mean residue ellipticity ($[\theta]_{MR}$) is expressed in degrees/cm^2/dmol.

Statistical Analysis

Statistical analysis using one-way ANOVA (Statistical Analysis System, SAS, version 6.03) was used to determine significant difference for various parameters. A significance level of $P < 0.05$ was used.

RESULTS

Peptide Synthesis

The HPLC profiles and mass spectra of the synthesized peptides are shown in Figure 1. The purities of all the peptides were above 96%. The identities of the peptides were confirmed by ESI-MS. The calculated molecular weights of apidaecin, Fl-K-apidaecin, AP1-9, F1-K-AP1-9, AP9-17, F1-K-AP9-17 and *E.coli* DnaK D-E helix were 1957.3, 2456.89, 1005.5, 1521.7, 1065.6, 1581.5 and 3624.7 respectively, and the molecular weights determined by ESI-MS were fitly equal to the data calculated.

Antibacterial Activity of Apidaecin and its Fragments

Fluorescein isothiocyanate chromophore has a marked effect on peptide activity if added directly to the *N*-terminus of peptide, so an extra positive charge (Lys) was added before fluorescein isothiocyanate chromophore and the peptides of Fl-K-apidaecin, F1-K-AP1-9; and F1-K-AP9-17 to minimize the loss of antibacterial activity [24,25]. No substantial change was observed when comparing the activities of labeled and unlabeled peptides toward *E. coli* K88, *E. coli* BL21 or *Agrobacterium tumefaciens* (Table 2). The MIC values of apidaecin against the bacterial strains tested are in line with the results of earlier studies [1]. AP1-9 and AP9-17 show hardly any antibacterial activity against any of the bacteria tested.

Table 2 *In vitro* antibacterial activity of apidaecin analogs discussed in the text

Peptides	MIC (expressed in μg/ml) against bacteria (1000 cfu/ml)			
	E. coli K88	*E. coli* BL21	*A. tumefaciens*	*B. subtilis*
Apidaecin	0.5	0.5	2.0	10.0
AP1-9	>10	>10	>10	>10
AP9-17	>10	>10	>10	>10
Fl-K-apidaecin	1.0	1.0	4.0	>10
Fl-K-AP1-9	>10	>10	>10	>10
Fl-K-AP9-17	>10	>10	>10	>10

DOI: 10.1002/psc

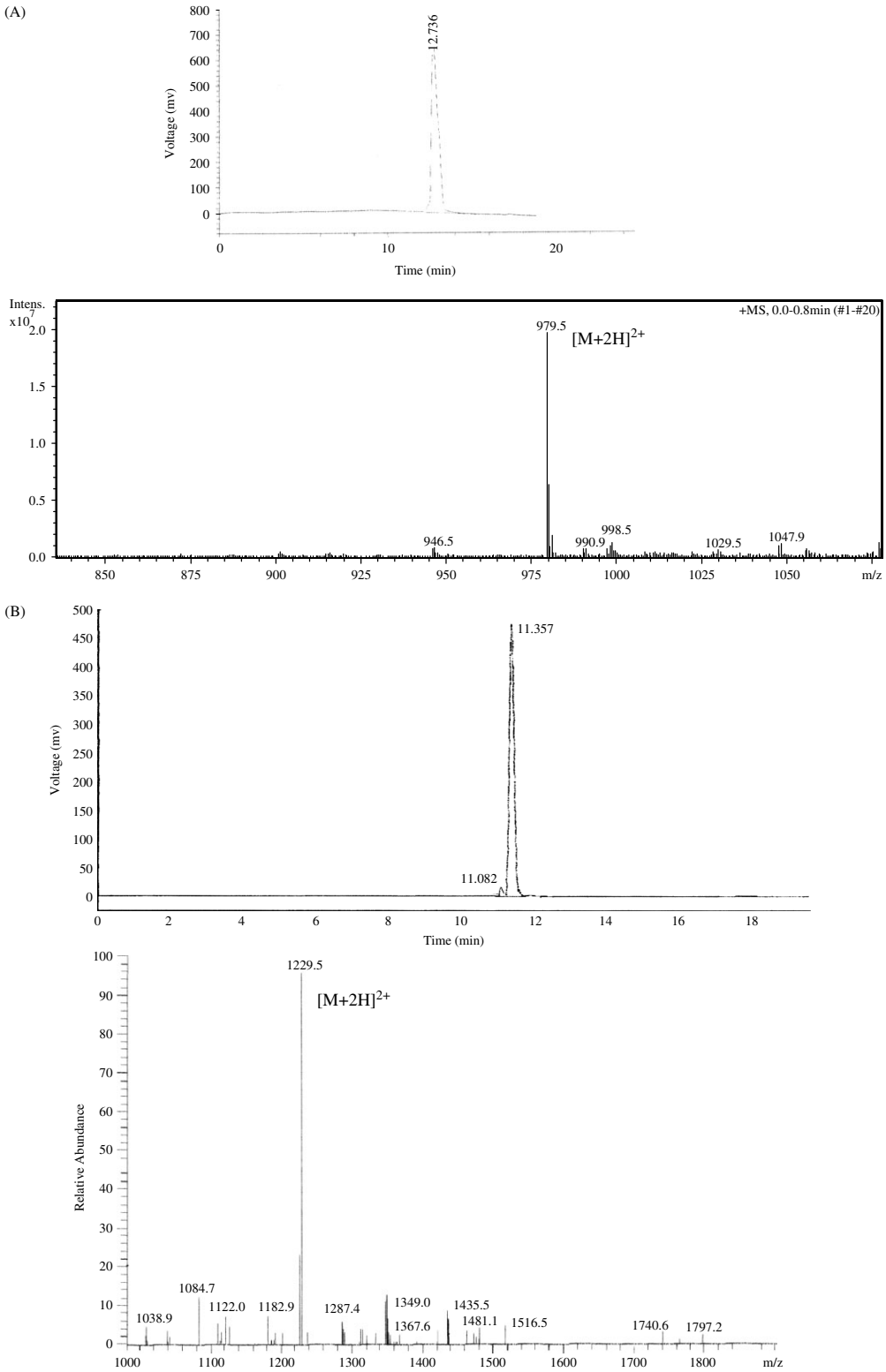

Figure 1 The HPLC profiles and ESI-MS analysis of the peptides synthesized in this study. The peptides are as follows: (A) Apidaecin, (B) Fl-K-apidaecin, (C) AP1-9, (D) F1-K-AP1-9, (E) AP9-17, (F) F1-K-AP9-17 and (G) *E.coli* DnaK D-E helix. The peptides were purified by semi-preparative HPLC on a C18 Vydac column (250 × 4.6 mm, 5 μm, 300 Å) (Amersham Pharmacia Biotech, Sweden). Apidaecin, AP1-9, AP9-17 and *E.coli* DnaK D-E helix fragment were eluted with a linear gradient of acetonitrile (15–45% v/v) in 0.1% TFA at 1.35% per minute. The flow rate was 1.0 ml/min and the absorbance of the eluate was monitored at 220 nm. Fl-K-apidaecin, Fl-K-AP1-9 and Fl-K-AP9-17 were eluted with a linear gradient of methanol (5–95% v/v) in 0.1% TFA at 2.0% per minute. The flow rate was 1.0 ml/min and the absorbance of the eluate was monitored at 490 nm. All the peptides were analyzed by ESI-MS using Bruker Esquire 3000plus ion trop mass spectrometer (Bruker-Franzen Analytik GmbH, Bremen, Germany). Instrument control and data acquisition were performed using Esquire 5.0 software.

DOI: 10.1002/psc

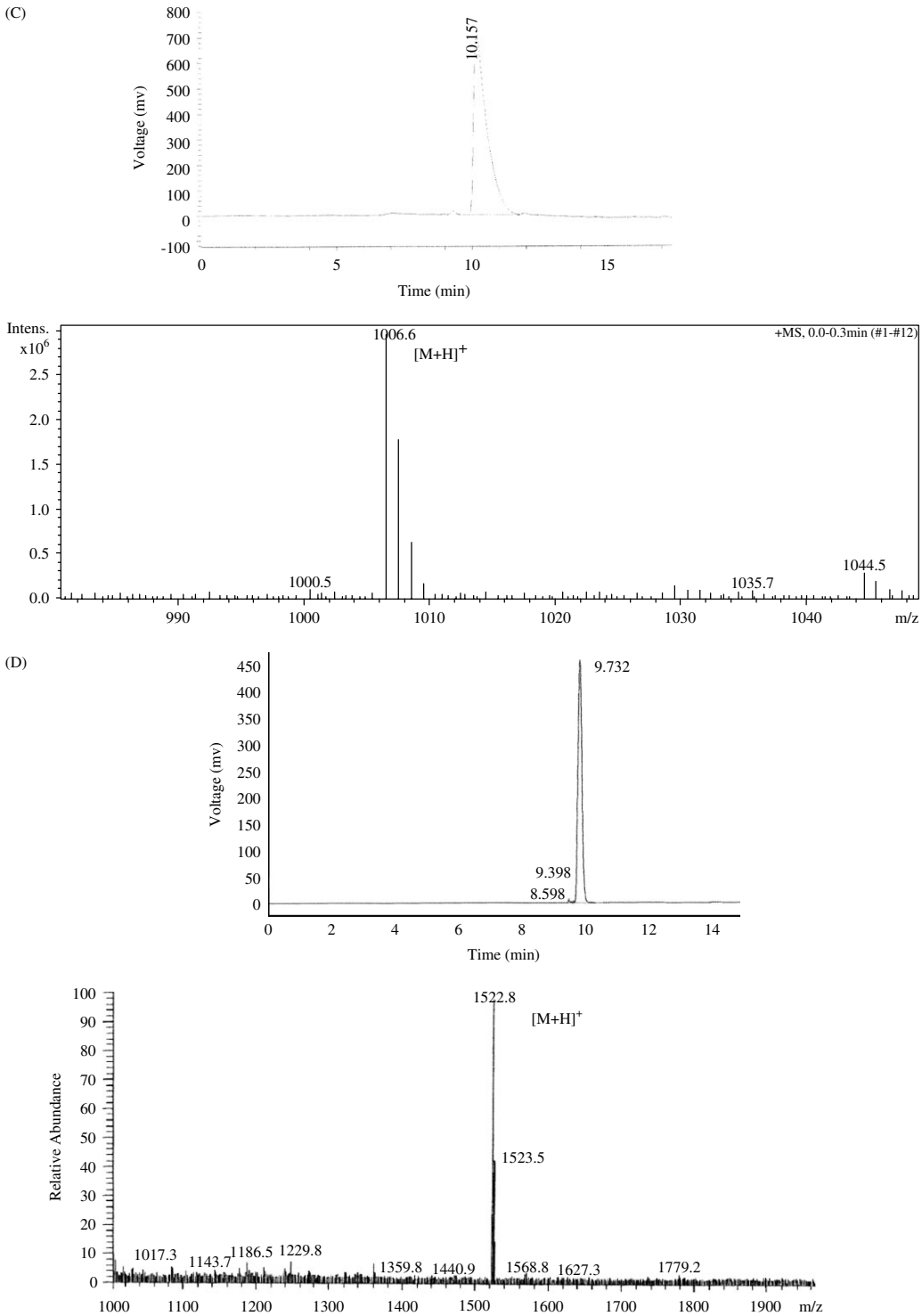

Figure 1 (*Continued*).

Peptide Entry into *E. coli* Cells

The proline-rich peptide has been proposed to have separate modules for cell entry and this has been proved for pyrrhocoricin [8]. So we studied the ability of apidaecin and its fragments to enter *E. coli* K88 cells to find out if apidaecin also has separate modules for cell entry. *N*-terminally labeled apidaecin, containing a lysine residue between the label and the antibacterial peptide, entered the bacterial cells very efficiently (Figure 2(A)). The staining appeared to be homogeneous throughout the cell (Figure 2(C)). Much weaker labeling of the *E. coli* cells was observed for the *N*-terminal 1–9 fragment (F1-K-AP1-9, Figure 2(B)) and the *C*-terminal 9–17 fragment (F1-K-AP9-17, Figure 2(D)).

DOI: 10.1002/psc

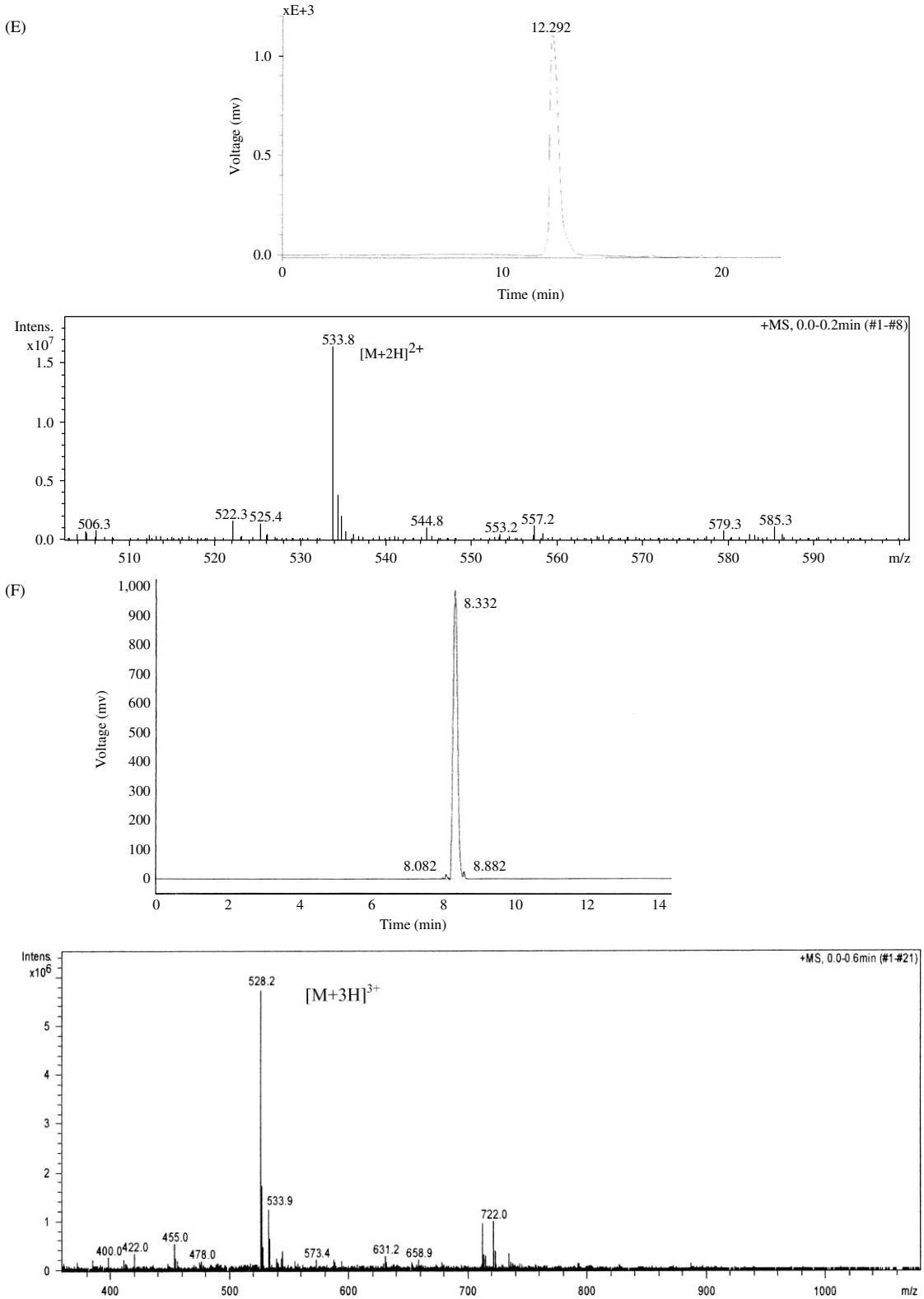

Figure 1 (*Continued*).

Inhibition of Protein Folding as Assayed by Enzyme Activity of Live *E. coli* Culture

It can be seen from Figure 3 that apidaecin inhibited the β-galactosidase and alkaline phosphatase activities of *E. coli* strain K88 culture significantly ($P < 0.05$, Figure 3, panel A, 83.18% for β-galactosidase; and panel B, 36.13% for alkaline phosphatase). AP1-9 inhibited the activities of both β-galactosidase and alkaline phosphates, but not significantly ($P > 0.05$).

DOI: 10.1002/psc

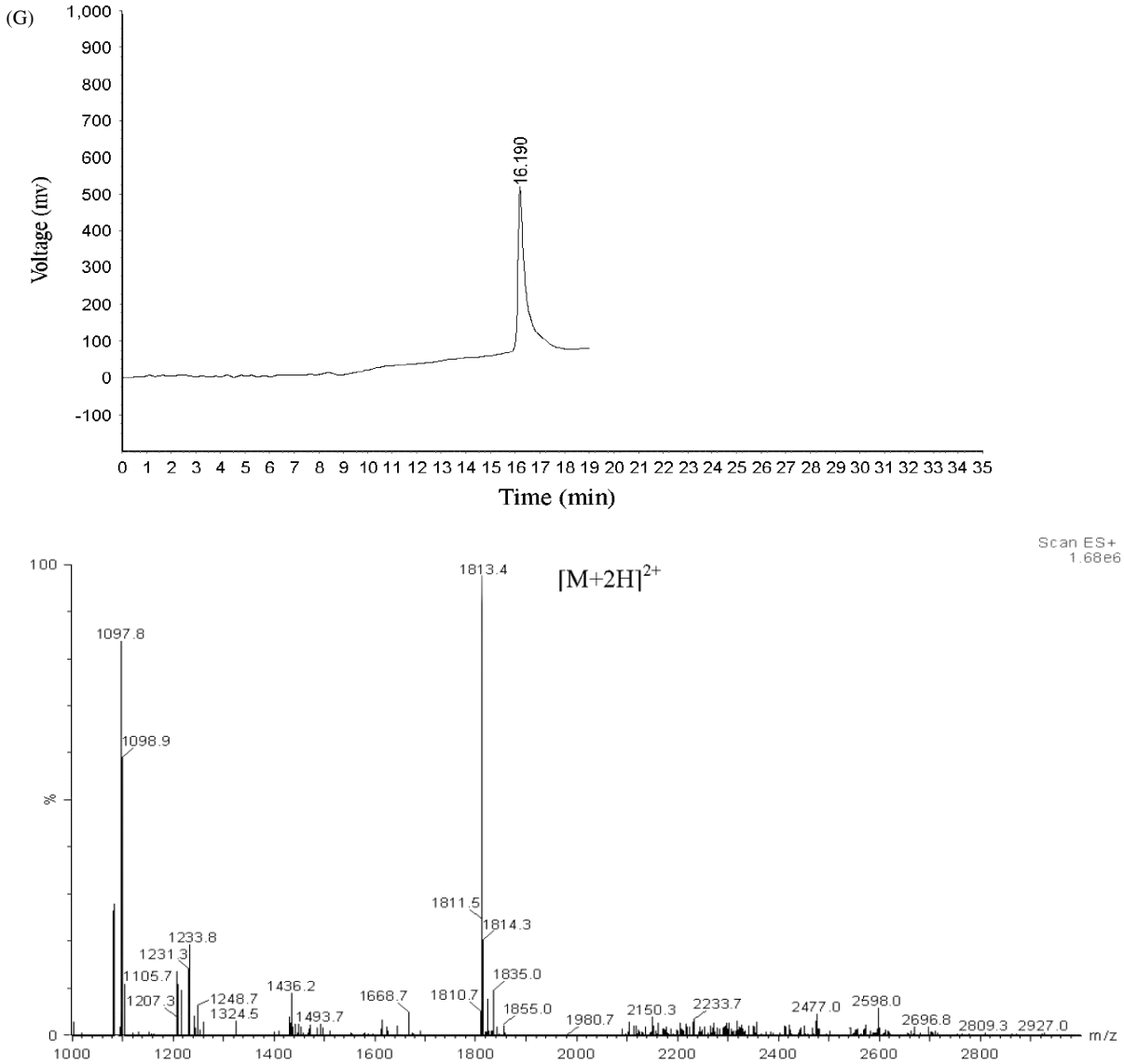

Figure 1 (*Continued*).

AP9-17 inhibited the β-galactosidase activity but increased the alkaline phosphatase activity slightly ($P > 0.05$). The negative control antimicrobial peptide magainin II, which is active against *E.coli* cells showed no effect on the activity of both enzymes. This excluded the possibility that β-galactosidase or alkaline phosphate activity was decreased by cell death. In the control experiment, apidaecin showed no significant effect on the activity of β-galactosidase or alkaline phosphatase when it was added to the bacteria supernatants containing these enzymes (data not shown).

ATPase Activity Assay

The assay was done in triplicate with the same DnaK protein. The results showed that apidaecin can greatly increase the ATPase activity of the *E. coli* DnaK protein (Figure 4) while AP1-9 and AP9-17 fragments both inhibited it.

Circular Dichroism (CD) Measurements

The CD curves of apidaecin and its fragments (Figure 5, panel A) indicated that the secondary structure of apidaecin contains neither α-helix nor β-sheet structures and there is lack of flexibility, while the characteristic poly-L-proline structure was evident, with a strong band between −200 and −210 nm, and a weak band between 210 and 230 nm [26]. To study the interaction of apidaecin with the lidless DnaK protein and the D-E helix fragment of DnaK, the CD curves of apidaecin, *E. coli* DnaK 583–615–apidaecin mixture and *E. coli* lidless DnaK–apidaecin mixture were measured. If the sum of the individual CD curves of the two interacting partners is different from that of the ligand–receptor mixture, this is a clear

DOI: 10.1002/psc

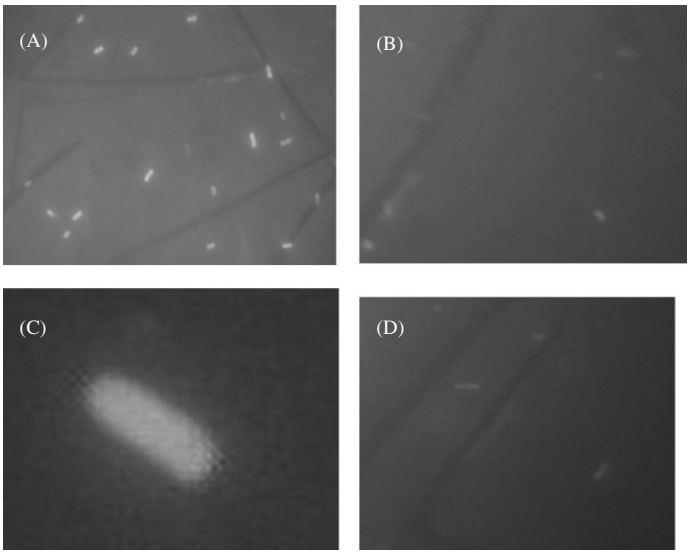

Figure 2 Confocal fluorescence microscopic images of *E. coli* K88 cells upon incubation with fluorescein-labeled apidaecin and its fragments. The peptide substrates are as follows: (A) and (C) Fl-K-apidaecin, (B) F1-K-AP1-9, and (D) F1-K-AP9-17. The final peptide concentration was 10 μg/ml for Fl-K-apidaecin, and 5.0 μg/ml for Fl-K-AP1-9 and Fl-K-AP9-17. In panels (B) and (D), apidaecin was also taken in by several cells, and this is a case thing.

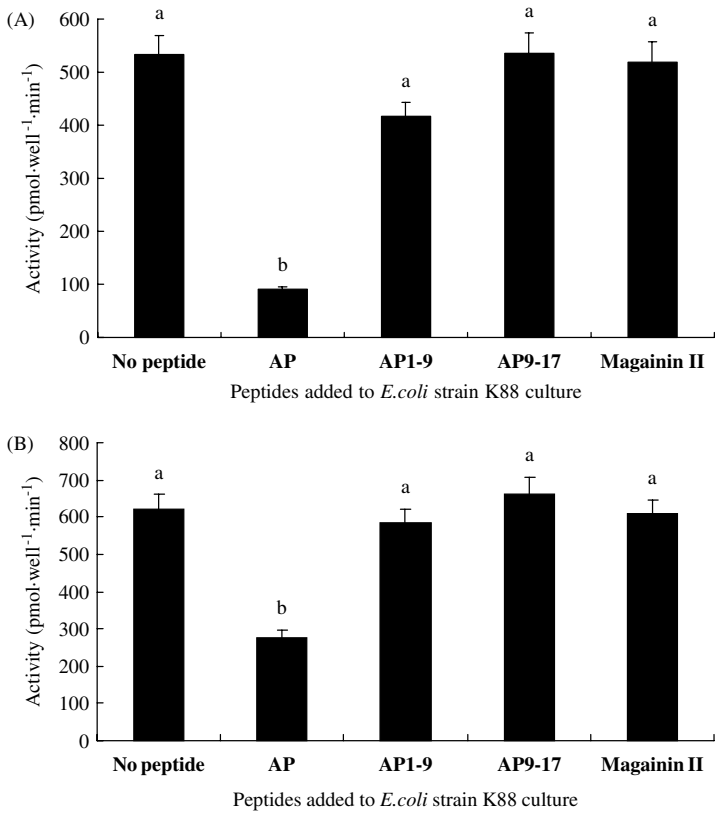

Figure 3 Effects of apidaecin and its fragments on β-galactosidase (panel A) and alkaline phosphatase (panel B) activity of *E. coli* cells. The experiments were done in triplicate with bacteria growing at different rates according to Kragol *et al* [8]. The peptides were added to the *E.coli* cultures at a concentration of 60 μg/ml for apidaecin, a value above the MIC of apidaecin, and 30 μg/ml for AP1-9 and AP9-17, about the same molarity as their active analog, apidaecin. The magainin II antimicrobial peptide which is active against *E.coli* cells was used as the negative control antimicrobial peptide. The concentration of magainin II was 20 μmol/ml, a value above the MIC. The average values are reported. When error bars are given in Figures, they represent the standard deviation.

DOI: 10.1002/psc

indication of binding and of a conformational change upon interaction [24]. Obvious spectral alteration was detected when apidaecin was added to the lidless DnaK (Figure 5, panel C), while no alteration was observed when it was added to DnaK D-E helix fragments (Figure 5, panel B).

DISCUSSION

Functional Domain Analysis of Apidaecins

It has been proposed that the pharmacophore delivery unit architecture is a general feature of the proline-rich antibacterial peptide family, which has been proved for pyrrhocoricin and drosocin. For pyrrhocoricin, the *N*-terminal half, residues 2–10, was the fragment that contained the active segment, and the *C*-terminal half, residues 11–20, were responsible for cell entry [9,27,28]. In the present study, we synthesized two fragments of apidaecin, AP1-9 and AP9-17, to study the functional domains. Study of fluorescein-labeled apidaecin and its fragments entering *E. coli* K88 cells showed that *N*-terminally labeled apidaecin entered the bacterial cells very efficiently, while neither F1-K-AP1-9 nor F1-K-AP9-17 could. This implies that deletion of the *C*-terminal or the *N*-terminal region would greatly hinder the entry of apidaecin into *E. coli* cells. Both terminal regions are essential, although the *C*-terminal region appears to be more important than the *N*-terminal region for intracellular delivery of apidaecin. This result will offer information about the structure–activity relationship with respect to the antimicrobial activity of antimicrobial peptides [29,30].

The Ultimate Apidaecin-Binding Site(s) of DnaK

The *E. coli* 70 kDa molecular chaperone DnaK functions cotranslationally and post-translationally to promote protein folding and to inhibit the formation of toxic protein aggregates [31–33]. In an ATP-dependent reaction cycle, DnaK attaches to a stretch of exposed hydrophobic residues on partially denatured proteins which bound in the conventional substract-binding site of DnaK and refolds the protein molecule in concert with DnaK-mediated ATP hydrolysis. The region responsible for ATPase action has been identified in

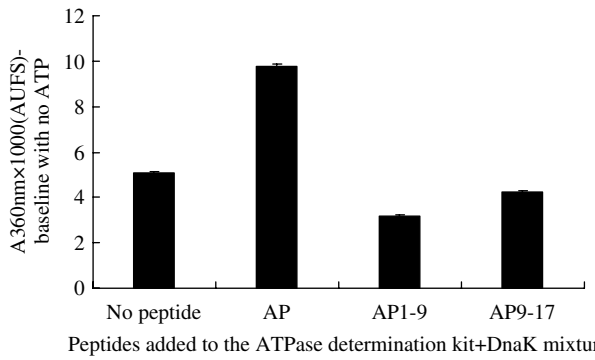

Figure 4 Effects of apidaecin on the ATPase activity of *E. coli* DnaK. A 5 μg portion of DnaK and 500 μM apidaecin, AP1-9 or AP9-17 were added to the EnzChek ATPase determination kit. The experiments were done in triplicate. The average values are reported.

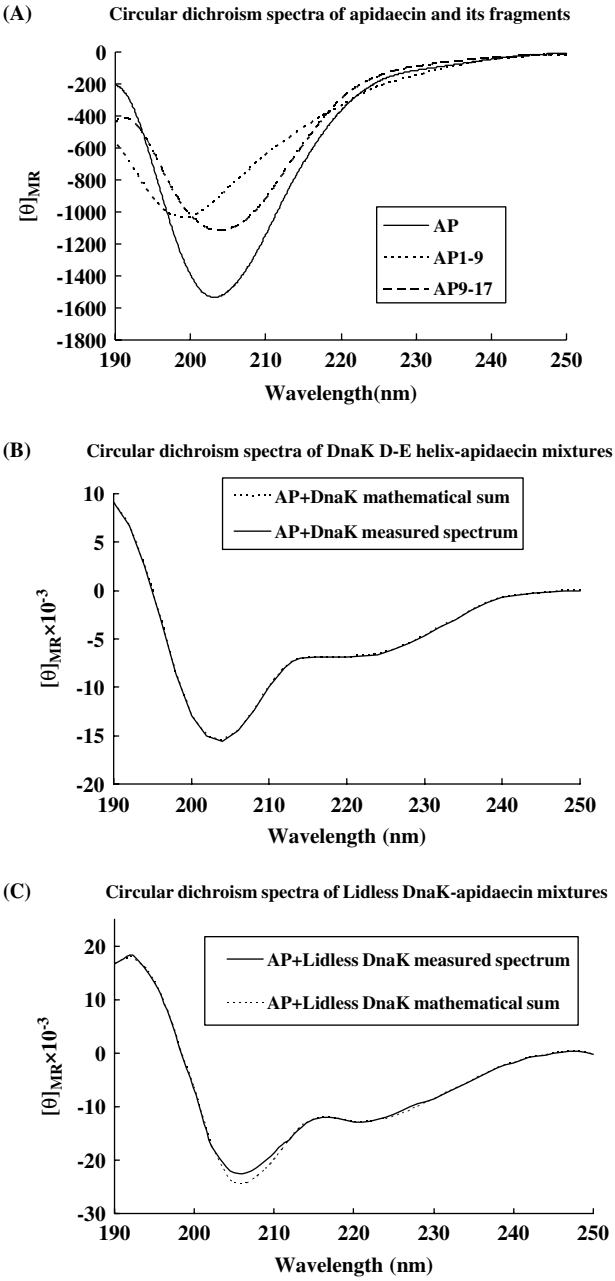

Figure 5 The CD spectra of apidaecin, AP1-19, and AP9-17 (panel A), *E. coli* DnaK helix D-E–apidaecin mixture (panel B) in water, and *E. coli* lidless DnaK–apidaecin mixture (panel C) in HEPES buffer. The spectra were taken at room temperature and the peptide concentration was approximately 1.0 mg/ml. In panel (B), the AP + DnaK mathematical sum curve (in point line) is almost invisible because it is covered by the measured one (in continuous line).

DOI: 10.1002/psc

the *N*-terminal half of the protein, the ATPase activity is modulated allosterically by the *C*-terminal domain of human Hsp70 and its analog [34]. The short proline-rich antibacterial peptides, including apidaecin, pyrrhocoricin, and drosocin, are proposed to bind specifically to the bacterial heat shock protein DnaK of *E. coli* [2]. There have been detailed studies of pyrrhocoricin, but there is some disagreement as to the specific binding site(s) of DnaK. According to one study, pyrrhocoricin binds to wild-type DnaK at two sites; the conventional substrate-binding site, and the αD and αE helices of the multi-helical lid [2,24], while a recent study proposed that pyrrhocoricin binds only to the conventional substrate-binding site of DnaK [35].

In the present study, we aimed to study the binding sites of apidaecin with the *E. coli* DnaK protein. Study of the CD curves showed that obvious spectral alteration was detected when apidaecin was added to the lidless DnaK while no alteration was observed when it was added to DnaK D-E helix fragments. This indicated that apidaecin could interact with the conventional substrate binging site of DnaK protein, but not with the DnaK D-E helix. Further studies on the effect of apidaecin on the ATPase activity of DnaK and the significant biological function of DnaK, i.e. the refolding of misfolded proteins, showed that apidaecin could stimulate the ATPase activity of DnaK protein and inhibit the activities of β-galactosidase and alkaline phosphatase of *E. coli* K88 strain. These results suggested that apidaecin displays antimicrobial activity by binding to the conventional substrate-binding site of DnaK, decreases the cellular concentration of DnaK by competing with natural substrates, and inhibits the β-galactosidase and alkaline phosphatase activities of *E. coli* strain K88.

Acknowledgements

This study was partially supported by the Zhejiang Provincial Scientific Program, China (No. 2005C22038). We thank Dr Yong Gao (Monsanto Company, St Louis, USA) for reviewing the original draft and for his many constructive comments.

REFERENCES

1. Castle M, Nazarian A, Yi SS, Tempst P. Analog lethal effects of apidaecin on *Escherichia coli* involve sequential molecular interactions with diverse targets. *J. Biol. Chem.* 1999; **274**: 32555–32564.
2. Otvos L Jr. Antimicrobial peptides isolated from insects. *J. Pept. Sci.* 2000; **6**: 497–511.
3. Levy O. Antimicrobial proteins and peptides: anti-infective molecules of mammalian leukocytes. *J. Leukoc. Biol.* 2004; **76**: 909–925.
4. Li WF, Ma GX, Zhou XX. Apidaecin-type peptides: biodiversity, structure-function relationships and mode of action. *Peptides* 2006; **27**: 2350–2359.
5. Zhu WL, Hahm KS, Shin SY. Cathelicidin-derived Trp/Pro-rich antimicrobial peptides with lysine peptoid residue (Nlys): therapeutic index and plausible mode of action. *J. Pept. Sci.* 2007; **13**: 529–535.
6. Taguchi S, Nakagawa K, Maeno M, Momose H. In vivo monitoring system for structure-function relationship analysis of the antibacterial peptide apidaecin. *Appl. Environ. Microbiol.* 1994; **60**: 3566–7352.
7. Taguchi S, Ozaki A, Nakagawa K, Momose H. Functional mapping of amino acid residues responsible for the antibacterial action of apidaecin. *Appl. Environ. Microbiol.* 1996; **62**: 4622–4655.
8. Kragol G, Lovas S, Varadi G, Condie BA, Hoffmann R, Otvos L Jr. The antibacterial peptide pyrrhocoricin inhibits the ATPase actions of Dnak and prevents chaperone-assisted protein folding. *Biochemistry* 2001; **40**: 3016–3026.
9. Bencivengo AM, Cudic M, Hoffmann R, Otvos L Jr. The efficacy of the antibacterial peptide, pyrrhocoricin, is finely regulated by its amino acid residues and active domains. *Lett. Pept. Sci.* 2001; **8**: 201–209.
10. Gordon YJ, Romanowski EG, McDermott AM. A review of antimicrobial peptides and their therapeutic potential as anti-infective drugs. *Curr. Eye. Res.* 2005; **30**: 505–515.
11. Werle M, Bernkop-Schnürch A. Strategies to improve plasma half life time of peptide and protein drugs. *Amino Acids* 2006; **30**: 351–367.
12. Zikou S, Koukkou AI, Mastora P, Sakarellos-Daitsiotis M, Sakarellos C, Drainas C, Panou-Pomonis E. Design and synthesis of cationic Aib-containing antimicrobial peptides: conformational and biological studies. *J. Pept. Sci.* 2007; **1**: 481–486.
13. Flouret G, Chaloin O, Borovickova L, Slaninova J. Design of novel bicyclic analogues derived from a potent oxytocin antagonist. *J. Pept. Sci.* 2006; **12**: 412–419.
14. Slepenkov SV, Witt SN. Kinetics of the reactions of the *Escherichia coli* molecular chaperone DnaK with ATP: Evidence that a three-step reaction precedes ATP hydrolysis. *Biochemistry* 1998; **37**: 1015–1024.
15. Slepenkov SV, Witt SN. Kinetic analysis of how DnaK's lid regulates interdomain coupling: DnaK's lid inhibits transition to the low affinity state. *Biochemistry* 2002; **41**: 12224–12235.
16. Fields GB, Noble RL. Solid phase synthesis utilizing 9-fluorenylmethyoxy-carbonyl amino acids. *Int. J. Pept. Protein Res.* 1990; **35**: 161.
17. Andrushchenko VV, Vogel HJ, Prenner EJ. Optimization of the hydrochloric acid concentration used for trifluoroacetate removal from synthetic peptides. *J. Pept. Sci.* 2007; **13**: 37–43.
18. Chan WC, White PD. *Fmoc solid Phase Peptide Synthesis: A Practical Approach*. Oxford University Press: New York, 2000; 4–121.
19. Thieriet N, Alsina J, Giralt E, Guibe F, Albericio F. Use of alloc-amino acids in solid-phase peptide synthesis. Tandem deprotection-coupling reactions using neutral conditions. *Tetrahedron Lett.* 1997; **38**: 7275–7278.
20. Rapaport D, Shai Y. Aggregation and organization of pardaxin in phospholipid membranes. *J. Biol. Chem.* 1992; **267**: 6502–6509.
21. Kaiser E, Colescott RL, Bossing CD, Cook PI. Color test for detection of terminal amino groups in the solid phase synthesis of peptides. *Anal. Biochem.* 1970; **34**: 595–598.
22. Ueckert JE, ter Steeg PF, Coote PJ. Synergistic antibacterial action of heat in combination with nisin and magainin II amide. *J. Appl. Microbiol.* 1998; **85**: 487–494.
23. Szendrei GI, Fabian H, Mantsch HH, Lovas S, Nyeki O, Schon I, Otvos L Jr. Aspartate-bond isomerization affects the major conformations of synthetic peptides. *Eur. J. Biochem.* 1994; **226**: 917–924.
24. Kragol G, Hoffmann R, Chattergoon MA, Lovas S, Cudic M, Bulet P, Condie BA, Rosengren KJ, Montaner LJ, Otvos L Jr. Identification of crucial residues for the antibacterial activity of the proline-rich peptide, pyrrhocoricin. *Eur. J. Biochem.* 2002; **269**: 4226–4237.

25. Tomasinsig L, Skerlavaj B, Papo N, Giabbai B, Shai Y, Zanetti M. Mechanistic and functional studies of the interaction of a proline-rich antimicrobial peptide with mammalian cells. *J. Biol. Chem.* 2006; **281**: 383–391.
26. Ruzza P, Calderan A, Guiotto A, Osler A, Borin G. Tat cell-penetrating peptide has the characteristics of a poly(proline) II helix in aqueous solution and in SDS micelles. *J. Pept. Sci.* 2004; **10**: 423–426.
27. Bulet P, Dimarcq JL, Hetru C, Lagueux M, Charlet M, Hegy G, Van Dorsselaer A, Hoffmann JA. A novel inducible antibacterial peptide of Drosophila carries an O- glycosylated substitution. *J. Biol. Chem.* 1993; **268**: 14893–14897.
28. Bulet P, Urge L, Ohresser S, Hetru C, Otvos L Jr. Enlarged scale chemical synthesis and range of activity of drosocin, an O-glycosylated antibacterial peptide from Drosophila. *Eur. J. Biochem.* 1996; **238**: 64–69.
29. Czajgucki Z, Andruszkiewicz R, Kamysz W. Structure activity relationship studies on the antimicrobial activity of novel edeine A and D analogues. *J. Pept. Sci.* 2006; **12**: 653–662.
30. Kluver E, Adermann K, Schulz A. Synthesis and structure-activity relationship of beta-defensins, multi-functional peptides of the immune system. *J. Pept. Sci.* 2006; **12**: 243–257.
31. Bukau B, Horwich AL. The hsp70 and hsp60 chaperone machines. *Cell* 2001; **92**: 351–366.
32. Slepenkov SV, Witt SN. The unfolding story of the *Escherichia coli* Hsp70 DnaK: is DnaK a holdase or an unfoldase? *Mol. Microbiol.* 2002; **45**: 1197–1206.
33. Hartl FU, Hayer-Hartl M. Molecular chaperones in the cytosol: from nascent chain to folded protein. *Science* 2002; **295**: 1852–1858.
34. Davis J, Voisine C, Craig E. Intragenic suppressors of Hsp70 mutants: interplay between the ATPase and peptide-binding domains. *Proc. Natl. Acad. Sci. U S A* 1999; **96**: 9269–9276.
35. Chesnokova LS, Slepenkov SV, Witt SN. The insect antimicrobial peptide, L-pyrrhocoricin, binds to and stimulates the ATPase activity of both wild-type and lidless DnaK. *FEBS Lett.* 2004; **565**: 65–69.

DOI: 10.1002/psc